New Materials, Compounds and Applications
Vol.9, No.1, 2025, pp.175-189
https://doi.org/10.62476/nmca.91175

THERMODYNAMIC STUDY OF THE $ZnAs_2$ AND Zn_3As_2 COMPOUNDS BY THE ELECTROMOTIVE FORCE MEASUREMENTS METHOD

A.R. Aghayeva[1*], D.M. Babanly[1,2], Y.I. Jafarov[3], E.J. Ahmadov[2], D.B. Tagiyev[2]

[1]French - Azerbaijani University (UFAZ), Azerbaijan State Oil and Industry University (ASOIU), Baku, Azerbaijan
[2]Institute of Catalysis and Inorganic Chemistry, Ministry of Science and Education, Baku, Azerbaijan
[3]Baku State University, Baku, Azerbaijan

Abstract. Zinc arsenides are promising semiconductors due to their natural abundance, unique electronic properties such as high carrier mobility and structural anisotropy and significant potential for advancing sustainable technologies. In light of discrepancies in existing literature and the growing relevance of these compounds, this study presents a thermodynamic investigation of $ZnAs_2$ and Zn_3As_2 within the temperature range of 300-440 K using the low-temperature electromotive force (EMF) method. Equilibrium samples from the $ZnAs_2$ + As and Zn_3As_2 + $ZnAs_2$ two-phase regions of the Zn-As system were utilized, with phase compositions confirmed by powder X-ray diffraction analysis. The experimental data enabled the calculation of partial molar functions of zinc in the alloys, as well as the standard thermodynamic functions of formation and standard entropies for $ZnAs_2$ and Zn_3As_2 compounds. A comparative analysis with previously reported data was conducted, providing insights into the thermodynamic behavior of zinc arsenides and improving the accuracy of existing knowledge.

Keywords: *EMF method, zinc arsenides, thermodynamic functions, Gibbs free energy, enthalpy, entropy.*

Corresponding Author: *A.R. Aghayeva, French - Azerbaijani University, Azerbaijan State Oil and Industry University (ASOIU), Baku, Azerbaijan, e-mail: aytekin_agayeva@mail.ru*

Received: *18 January 2025;* ***Accepted:*** *10 March 2025;* ***Published:*** *9 April 2025.*

1. Introduction

Fundamental thermodynamic research plays a crucial role in advancing understanding of material properties and behaviors, providing essential insights that can guide both theoretical and practical applications. In the context of materials science, such research allows for the precise determination of phase equilibria, stability regions and the underlying thermodynamic parameters that govern the formation and transformation of compounds. For materials like zinc arsenides, thermodynamic studies offer valuable data on enthalpy, entropy and Gibbs free energy, which are essential for predicting their stability, reactivity and potential applications in various technological fields. By establishing a solid thermodynamic foundation, this research not only aids in the

How to cite (APA):
Aghayeva, A.R., Babanly, D.M., Jafarov, Y.I., Ahmadov, E.J. & Tagiyev, D.B. (2025). Thermodynamic study of the $ZnAs_2$ and Zn_3As_2 compounds by the electromotive force measurements method. *New Materials, Compounds and Applications*, *9*(1), 175-189 https://doi.org/10.62476/nmca.91175

optimization of existing materials but also opens the door to the design of new materials with tailored properties, ultimately contributing to advancements in areas such as energy storage, electronics and catalysis.

Metal arsenides represent an important class of materials known for their distinctive electronic, optical and physical properties. These compounds, formed through the combination of metals with arsenic, exhibit semiconducting behavior, making them invaluable for a wide range of advanced technological applications. Despite their inherent toxicity, metal arsenides play a crucial role in the development of optoelectronic devices, thermoelectric materials, photovoltaic technologies etc. Their direct band gaps enable efficient light absorption and emission, which is essential for applications in lasers, light-emitting diodes and infrared detectors (Buschow & Cahn, 2001; Vurgaftman *et al*., 2001; Ali *et al*., 2024; Crow *et al*., 1978; Jalali *et al*., 2022).

Among various metal arsenides, zinc arsenides have garnered considerable attention in materials science due to their unique physical properties, positioning them as promising candidates for diverse applications. A comprehensive understanding of their thermodynamic properties is crucial for optimizing both their synthesis and functional performance in technological contexts. Thermodynamic investigations offer valuable insights into the stability, phase transitions and reaction mechanisms of these materials, thereby facilitating precise control over their fabrication and tailored properties (Kim *et al*., 2024; Burgess *et al*., 2015; Stoyko *et al*., 2011; Colegrove *et al*., 2020; Galstyan *et al*., 1991).

Zinc diarsenide $ZnAs_2$ is a direct bandgap semiconductor that belongs to the broader category of $A^{II}B^{V}$ compounds which are of significant interest for both fundamental research and practical applications. A distinctive characteristic of this phase is the coexistence of As-As bonds alongside Zn-As bonds, forming zigzag chains aligned along the c axis. This structural feature significantly contributes to its anisotropic electronic properties, which are highly beneficial for device fabrication. The electrical and optical properties of zinc diarsenide have been extensively studied and documented in numerous reviews (Stamov *et al*., 2012; 2022; Rajpurohit & Sharma; 2023; Islam & Kauzlarich, 2023; Khan *et al*., 2022; Kozlov *et al*., 2002).

Zn_3As_2 is a promising p-type semiconductor characterized by high effective mobility. Its abundance in the Earth's crust, combined with its advantageous electronic properties, further enhances its potential for sustainable and cost-effective technologies. With a bandgap of approximately 1 eV, Zn_3As_2 is particularly well-suited for optoelectronic applications, including infrared detection and energy conversion. This versatility not only enhances its potential for use in advanced optoelectronic devices but also positions it as an attractive candidate for cost-effective and sustainable technological solutions (Stutz *et al*., 2019; Hnuna *et al*., 2023; Kaur *et al*., 2020; Kim *et al*., 2024; Zakhvalinskii *et al*., 2021; Sicius *et al*., 2024).

The phase diagram of the Zn-As system has been studied by several authors, results of which were summarized by Okamoto (1992). There are two stoichiometric phases in the system. Both of them, namely, $ZnAs_2$ and Zn_3As_2 melt congruently at 1043 and 1288 K, respectively. The $ZnAs_2$ phase has a narrow homogeneity range between 33.0 and 33.5 at. % Zn (Lazarev *et al*., 1979). The Zn_3As_2 phase undergoes two polymorphic transformations: β- Zn_3As_2 ↔ α′- Zn_3As_2 at 924 K and α′- Zn_3As_2 ↔ α- Zn_3As_2 at 463 K (Okamoto, 1992). The solubility of As in α- Zn_3As_2 does not exceed $5 \cdot 10^{-4}$ at. % (Lazarev *et al*., 1981).

In recent years, computational methods have been employed to perform thermodynamic assessments of the Zn-As system (Kidari & Chartrand, 2023; Ghasemi & Johansson, 2015), with the results showing significant agreement with the data reported in (Okamoto, 1992). Consequently, this study utilizes the phase diagram of the Zn-As system as presented in (Okamoto, 1992).

A comprehensive understanding of the thermodynamics and phase behavior of the Zn-As system is critical for reducing the environmental impact of these materials, particularly in industries focused on metal refining and waste management. Thermodynamic study of zinc arsenides has been previously carried out by several authors and their results have been summarized in different contemporary review articles and databases (Iorish & Yungman, 2006; Barin, 2008; Kubaschewski *et al*., 1967; Wagman *et al*., 1967; Sirota & Sklyarenko, 1968; Binnewies & Milke, 2002). Initial analysis of literary data has shown that the results of thermodynamic study of zinc arsenides are scattered and inconsistent. Later on, at the discussions section of the paper, the results of those studies will be discussed, focusing on experimental methods and models that have been used to estimate related thermodynamic properties and will be compared with the ones obtained in current study.

Considering above, present contribution is dedicated to the thermodynamic study of zinc antimonides by the low temperature EMF measurements.

Various modifications of the EMF method are commonly employed for the thermodynamic analysis of binary and more complex inorganic systems. Depending on different factors such as chemical compatibility with the electrodes, stability and non-reactivity within the system and suitability for the temperature range being studied etc., different types of liquid and solid electrolytes can be applied for EMF measurements (Isper *et al*., 2010; Nigl *et al*., 2017; Babanly *et al*., 2024; 2025; Mashadieva *et al*., 2021a; 2021b; Aliyev *et al*., 2024; 2010; Babanly *et al*., 2009; Aliyev *et al*., 2010; Aliev *et al*., 2018; Babanly *et al*., 2019; Moroz *et al*., 2024).

2. Experimental part

Selection of the synthesized samples, as well as their preparation and thermal annealing conditions, was guided referring the phase diagram of the Zn-As system (Okamoto, 1992). Alloys from the $ZnAs_2$ + As and Zn_3As_2 + $ZnAs_2$ two-phase regions were specifically chosen to examine the thermodynamic properties of zinc arsenides. For the thermodynamic study of $ZnAs_2$ and Zn_3As_2 compounds, samples with 73 and 80 at.% As composition from the $ZnAs_2$ + As region and those with 50 and 60 at.% As composition from the Zn_3As_2 + $ZnAs_2$ region were utilized, respectively.

High-purity elements (zinc lumps - Sigma-Aldrich, CAS number 7440-66-6 and arsenic pieces - Alfa-Aesar, CAS number 7440-38-2) were used for sample preparation. For synthesis, precise quantities of elements were measured using an analytical balance and placed into quartz ampoules. The total mass of each sample was 1 gram. The ampoules were evacuated to a pressure of about 10^{-2} Pa and heated to 1100 K. Synthesis was carried out around 3-5 hours, ampoules cooled down to 750 K and were kept at this temperature for ~100 hours. Subsequently, the temperature was lowered to the experimental range and stabilized at 400 K, where it was held for an additional 100 hours to ensure equilibrium.

The phase composition of the synthesized equilibrium alloys was verified through powder X-ray diffraction (PXRD) analysis. The measurements were performed at room temperature using a D2 Phaser diffractometer with CuKα radiation, scanning within an

angular range of approximately 5° to 75°. The resulting diffraction patterns were analyzed with the Topas 4.2 profile modeling software.

The diffraction pattern of one sample from each phase region is represented in Figure 1. As can be seen, the PXRD spectrum of the sample with 73 at. % As composition (Figure 1a) is composed of the diffraction peaks of simple antimony and $ZnAs_2$, while the one for the sample with 50 at. % As composition (Figure 1b) consists of the diffraction lines of $ZnAs_2$ and Zn_3As_2. PXRD analysis showed no signals indicative of additional phases in samples, confirming successfully completion of synthesis process and the phase compositions of alloys being in alignment with the T-x phase diagram of the system under study (Okamoto, 1992).

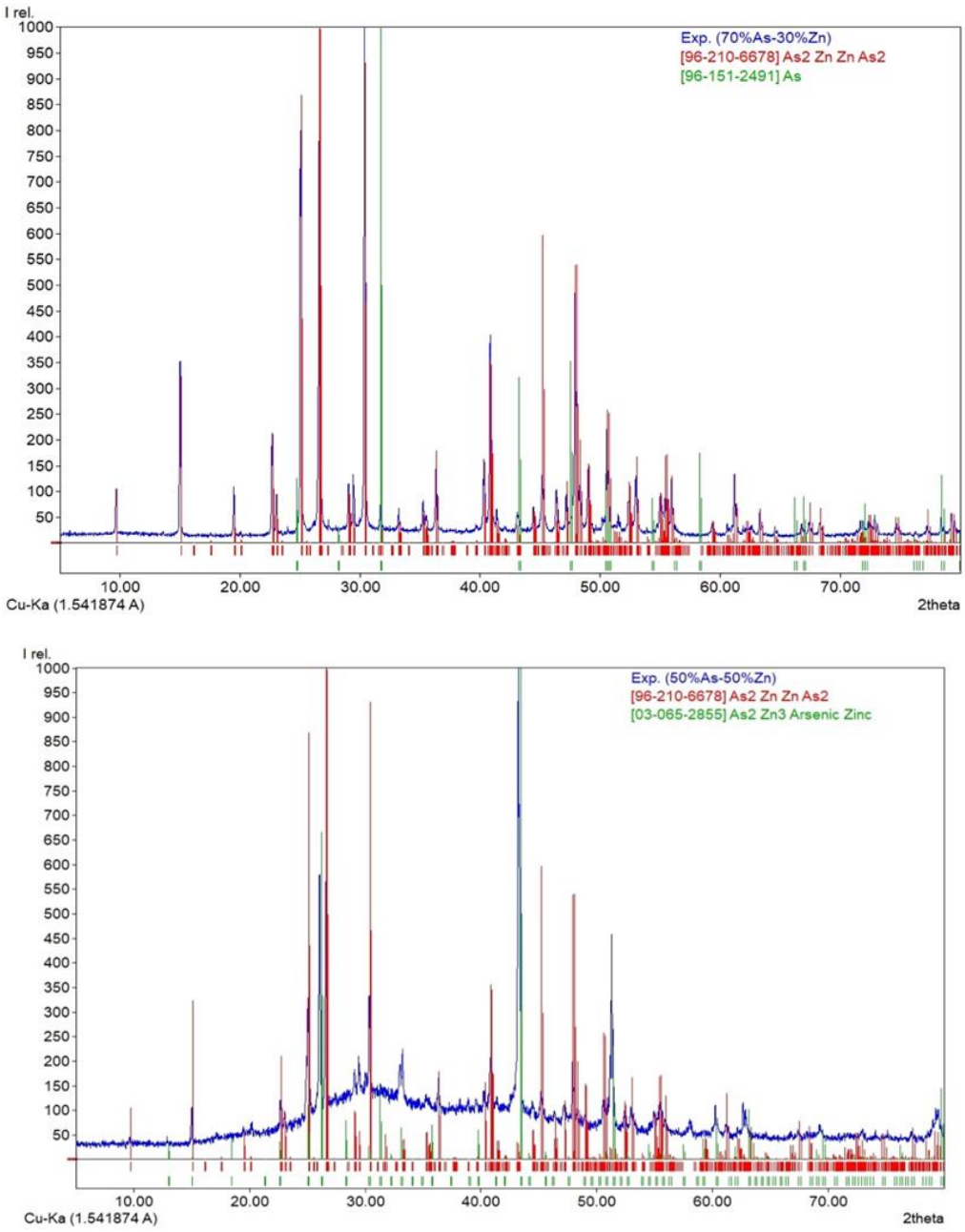

Figure 1. Powder X-ray diffraction patterns of the samples taken from the $ZnAs_2$ + As and $ZnAs_2$ + Zn_3As_2 phase regions of the Zn-As binary system with: a) 73 at. % As and b) 50 at. % As composition

To perform the EMF measurements, the following electrochemical setup was assembled:

$$(-)\ Zn(s) / glycerol + KCl + ZnCl_2 / Zn\text{-}As\ alloy\ (s)\ (+) \qquad (1)$$

The more reactive element of the system, zinc, was selected as the left electrode. Four equilibrium alloys with specified compositions were used as the right electrodes. After synthesis and annealing, the alloys were ground into powder and pressed into tablets with diameters of 5-6 mm. These tablets were then mounted onto molybdenum rods, which, along with the electrodes, were coated with glass to prevent unintended contact with the electrolyte solution.

The liquid electrolyte used in the assembled cell was composed of a glycerol solution with small amounts of anhydrous KCl and $ZnCl_2$ salts added. Glycerol was chosen as the electrolyte in our study due to its unique properties that make it particularly suitable for EMF measurements. Glycerol has a high dielectric constant, low volatility and good thermal stability, which ensures consistent and reliable measurements over a wide range of temperatures. Additionally, glycerol's non-reactivity with the studied compounds minimizes the risk of contamination or unwanted side reactions during the experiment. These advantages make glycerol an ideal medium for conducting precise and reproducible EMF measurements. Moreover, compared to other electrolytes, glycerol provides a stable environment for the electrochemical processes involved, ensuring more accurate thermodynamic data.

The inclusion of KCl enhances the ionic conductivity of the electrolyte and stabilizes it by maintaining a suitable ionic strength, thereby minimizing significant fluctuations in ion concentration during the EMF measurements. In thermodynamic studies of zinc arsenides, $ZnCl_2$ was also added to the glycerol-based electrolyte as a source of Zn^{+2} ions. This addition ensures a stable electrochemical environment, facilitating accurate EMF measurements. To remove moisture and oxygen, the glycerol was meticulously dehydrated and degassed under a dynamic vacuum at approximately 350 K. The preparation of the electrolyte and electrodes, along with the assembly of the electrochemical cell (1), adhered to the procedures described in references (Morachevsky *et al*., 2003; Shao, 2012; Babanly *et al*., 2011; Babanly *et al*., 2011).

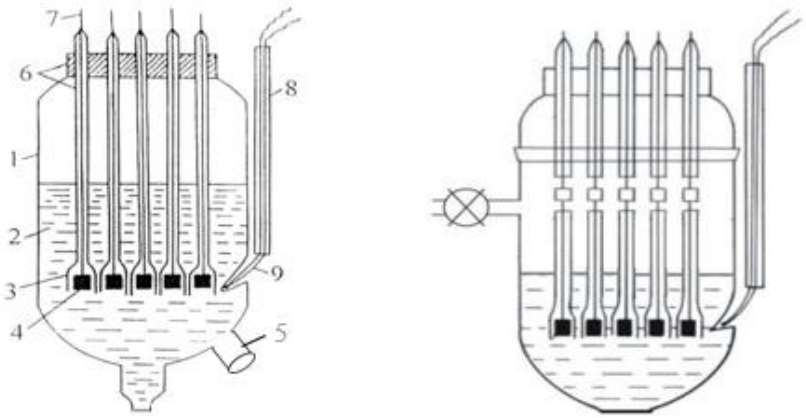

Figure 2. Electrochemical cell used for EMF measurements in liquid electrolyte concentration cells: a) for single-use; b) for numerous experiments: 1-pyrex pot, 2-electrolyte, 3-protective glass cover, 4-alloy electrode, 5-soldering, 6-glass capillaries, 7-molybdenum wires, 8-thermocouple ceramic coating, 9-thermocouple

The schematic diagram of the electrochemical cell applied inj current study is presented in Figure 2. This setup enables the simultaneous measurement of multiple (3-5) samples.

Note that, the EMF method offers high sensitivity, non-destructive measurements and direct determination of thermodynamic quantities like Gibbs free energy, entropy and enthalpy. It is cost-effective, requires minimal sample preparation, can be applied over a wide temperature range and is versatile for various materials, making it an efficient tool for thermodynamic studies.

3. Results and discussions

Experimental measurements showed that the EMF values remained constant within the both two-phase regions, regardless of the overall composition of the electrode alloys. The temperature dependence of the EMF values for these alloys was found to be nearly linear (Figure 3 a, b). This linear relationship further validates the stability of the compositions of the coexisting phases within these heterogeneous regions across the studied temperature range. Moreover, it establishes a foundation for calculating the partial entropy and enthalpy, utilizing the temperature coefficients of the EMF (Shao, 2012; Babanly *et al*., 2011). This enabled the interpretation of the experimental E and T data through least-squares fitting using Microsoft Office Excel software. The calculation procedures for both phase regions are outlined in Tables 1 and 2.

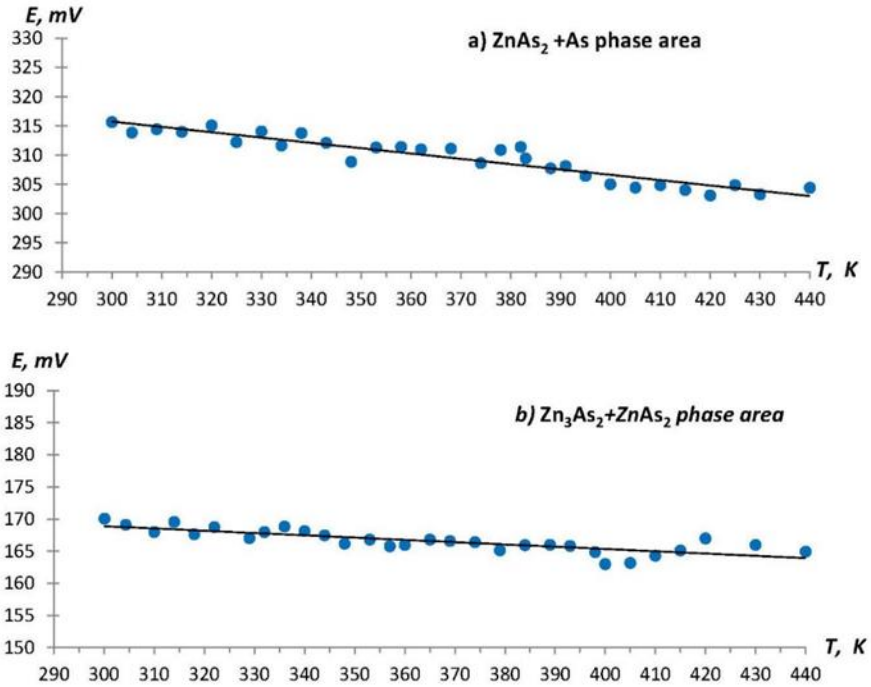

Figure 3. Dependencies of the experimental EMF (E, mV) values on temperature (T, K) for the samples taken from the a) $ZnAs_2$ + As and b) $ZnAs_2$ + Zn_3As_2 phase areas of the Zn-As system

Thus, analysis of the collected experimental data yields the linear equations of the following type (Babanly *et al*., 2019; Moroz *et al*., 2024).

$$E = a + bT \pm t \cdot \left[\frac{\delta_E^2}{n} + \delta_b^2 (T - \overline{T})^2 \right]^{1/2} \quad (2)$$

where a and b are constant coefficients, n is the number of pairs of experimental E and T values; δ_E^2 and δ_b^2 are the error variances of the EMF readings and b coefficient, respectively; $\overline{T}$ is the average of the absolute temperature; t is Student's test. At a confidence level of 95% and a number of experimental points n=30, the Student's criterion is t=2.045 ≈ 2.0.

Table 1. Computer-processed experimental E and T data by implementation of the least squares method for alloys taken from the $ZnAs_2$ +As phase area of the Zn-As system

T_i K	E_i mV	$T_i - \overline{T}$ K	$E_i (T_i - \overline{T})$ mV·K	$(T_i - \overline{T})^2$ K^2	$\breve{E}$ mV	$E_i - \breve{E}$ mV	$(E_i - \breve{E})^2$ mV^2
300,1	**315,66**	-68,07	-21485,92	4633,07	315,77	-0,11	0,01
304,4	**313,87**	-64,07	-20108,60	4104,54	315,41	-1,54	2,37
309,1	**314,44**	-59,07	-18572,92	3488,87	314,96	-0,52	0,27
314,3	**314,01**	-54,07	-16977,47	2923,20	314,50	-0,49	0,24
320,2	**315,07**	-48,07	-15144,36	2310,40	313,95	1,12	1,25
325,1	**312,23**	-43,07	-13446,71	1854,74	313,50	-1,27	1,61
330,4	**314,06**	-38,07	-11955,22	1449,07	313,04	1,02	1,03
334,2	**311,66**	-34,07	-10617,22	1160,54	312,68	-1,02	1,04
338,3	**313,76**	-30,07	-9433,72	904,00	312,32	1,44	2,09
343,1	**312,12**	-25,07	-7823,81	628,34	311,86	0,26	0,07
348,2	**308,88**	-20,07	-6198,19	402,67	311,40	-2,52	6,38
353,3	**311,30**	-15,07	-4690,25	227,00	310,95	0,35	0,12
358,4	**311,41**	-10,07	-3134,86	101,34	310,49	0,92	0,84
362,1	**310,98**	-6,07	-1886,61	36,80	310,13	0,85	0,72
368,2	**311,12**	-0,07	-20,74	0,00	309,58	1,54	2,36
374,2	**308,63**	5,93	1831,20	35,20	309,04	-0,41	0,17
378,1	**310,90**	9,93	3088,27	98,67	308,67	2,23	4,95
382,3	**311,41**	13,93	4338,98	194,14	308,31	3,10	9,61
383,2	**309,45**	14,93	4621,12	223,00	308,22	1,23	1,52
388,5	**307,76**	19,93	6134,68	397,34	307,76	0,00	0,00
391,1	**308,12**	22,93	7066,22	525,94	307,49	0,63	0,40
395,2	**306,44**	26,93	8253,45	725,40	307,13	-0,69	0,47
400,3	**305,02**	31,93	9740,31	1019,74	306,67	-1,65	2,73
405,1	**304,45**	36,93	11244,35	1364,07	306,22	-1,77	3,12
410,2	**304,88**	41,93	12784,63	1758,40	305,76	-0,88	0,78
415,1	**304,03**	46,93	14269,14	2202,74	305,31	-1,28	1,63
420,3	**303,11**	51,93	15741,51	2697,07	304,85	-1,74	3,03
425,1	**304,85**	56,93	17356,13	3241,40	304,40	0,45	0,21
430,2	**303,31**	61,93	18785,00	3835,74	303,94	-0,63	0,40
440,1	**304,42**	71,93	21897,95	5174,40	303,03	1,39	1,93
$\overline{T}$ =368.07	**$\overline{E}$ =309.58**		**∑ = -4343.67**	**∑= 47717.87**			**∑ = 51.32**

Table 2. Computer-processed experimental E and T data by implementation of the least squares method for alloys taken from the $ZnAs_2$ + Zn_3As_2 phase area of the Zn-As system

T_i K	E_i mV	$T_i - \overline{T}$ K	$E_i\,(T_i - \overline{T})$ $mV \cdot K$	$(T_i - \overline{T})^2$ K^2	$\breve{E}$ mV	$E_i - \breve{E}$ mV	$(E_i - \breve{E})^2$ mV^2
300,1	**170,08**	-64,51	-10972,43	4161,97	168,91	1,17	1,38
304,3	**169,11**	-60,31	-10199,59	3637,70	168,76	0,35	0,12
310,1	**167,99**	-54,61	-9174,49	2982,62	168,55	-0,56	0,32
314,4	**169,55**	-50,61	-8581,49	2561,71	168,41	1,14	1,30
318,2	**167,63**	-46,61	-7813,79	2172,80	168,27	-0,64	0,41
322,3	**168,73**	-42,61	-7190,15	1815,90	168,13	0,60	0,36
329,1	**167,03**	-35,61	-5948,50	1268,31	167,88	-0,85	0,72
332,2	**167,99**	-32,61	-5478,71	1063,63	167,77	0,22	0,05
336,3	**168,83**	-28,61	-4830,79	818,72	167,63	1,20	1,45
340,5	**168,14**	-24,61	-4138,49	605,82	167,48	0,66	0,43
344,4	**167,46**	-20,61	-3451,91	424,91	167,34	0,12	0,01
348,1	**166,17**	-16,61	-2760,64	276,00	167,20	-1,03	1,06
353,1	**166,82**	-11,61	-1937,34	134,87	167,02	-0,20	0,04
357,3	**165,76**	-7,61	-1261,99	57,96	166,88	-1,12	1,25
360,2	**165,97**	-4,61	-765,67	21,28	166,77	-0,80	0,64
365,1	**166,82**	0,39	64,50	0,15	166,59	0,23	0,05
369,5	**166,57**	4,39	730,69	19,24	166,45	0,12	0,01
374,3	**166,41**	9,39	1562,04	88,11	166,27	0,14	0,02
379,1	**165,12**	14,39	2375,53	206,98	166,10	-0,98	0,95
384,5	**165,93**	19,39	3216,83	375,84	165,92	0,01	0,00
389,6	**165,99**	24,39	4047,94	594,71	165,74	0,25	0,06
393,1	**165,81**	28,39	4706,79	805,80	165,60	0,21	0,05
398,2	**164,88**	33,39	5504,79	1114,67	165,42	-0,54	0,29
400,3	**163,00**	35,39	5768,03	1252,22	165,35	-2,35	5,51
405,4	**163,17**	40,39	6589,89	1631,08	165,17	-2,00	4,00
410,1	**164,28**	45,39	7456,12	2059,95	164,99	-0,71	0,51
415,3	**165,11**	50,39	8319,34	2538,82	164,81	0,30	0,09
420,1	**166,99**	55,39	9249,02	3067,68	164,63	2,36	5,55
430,3	**165,98**	65,39	10852,88	4275,42	164,28	1,70	2,90
440,2	**164,92**	75,39	12432,77	5683,15	163,92	1,00	1,00
$\overline{T}$ =364.61	**$\overline{E}$ =166.61**		**$\sum$ = -1628.81**	**$\sum$= 45718.01**			**$\sum$ = 30.51**

Obtained linear equations of the type (2) are presented in Table 3. Based on these linear equations and using the thermodynamic expressions below given, the partial molar Gibbs free energy, enthalpy and entropy of cadmium in alloys have been calculated (Moroz *et al*., 2024; Morachevsky *et al*., 2003; Shao, 2012; Babanly *et al*., 2011; Babanly *et al*., Babanly & Yusibov, 2011) :

$$\Delta\overline{G}_{Zn} = -zFE \tag{3}$$

$$\Delta\overline{S}_{Zn} = zF\left(\frac{\partial E}{\partial T}\right)_P = zFb \tag{4}$$

$$\Delta\overline{H}_{Zn} = -zF\left[E - T\left(\frac{\partial E}{\partial T}\right)_P\right] = -zFa \tag{5}$$

where ***z*** is the number of electrons involved in the reaction and ***F*** is Faraday's **constant** (96,485 J/mol). Obtained relative partial molar functions of zinc in alloys are presented in Table 4.

Table 3. Linear equations derived from the processing of experimental data for the $ZnAs_2$ + As and Zn_3As_2 + $ZnAs_2$ phase areas of the Zn-As binary system

Phase region	*E, mV = a + bT ± 2S$_E$ (T)*
$ZnAs_2$ + As	$343.08 - 0.0910\,T \pm 2\left[\frac{1.71}{30} + 3.6 \cdot 10^{-5}(T - 368.1)^2\right]^{1/2}$
Zn_3As_2 + $ZnAs_2$	$179.6 - 0.0356\,T \pm 2\left[\frac{1.02}{30} + 2.2 \cdot 10^{-5}(T - 364.6)^2\right]^{1/2}$

Table 4. Relative partial molar Gibbs free energy, enthalpy and entropy of zinc in the alloys of the Zn-As system at 298 K

Phase region	$-\Delta\overline{G}_{Zn}$	$-\Delta\overline{H}_{Zn}$	$\Delta\overline{S}_{Zn}$
	kJ · mol^{-1}		*J · mol^{-1} · K^{-1}*
$ZnAs_2$ + As	60.97 ± 0.09	66.21 ± 0.43	- 17.57 ± 1.16
Zn_3As_2 + $ZnAs_2$	32.61 ± 0.07	34.66± 0.33	- 6.88 ± 0.91

According to the phase diagram of the Zn-As binary system (Okamoto, 1992), the partial molar functions of zinc in the $ZnAs_2$ + As and Zn_3As_2 + $ZnAs_2$ two-phase fields (Table 4) are thermodynamic functions of the following virtual-cell reactions, correspondingly:

$$Zn\ (s) + 2\ As\ (s) = ZnAs_2\ (s) \quad (6)$$

$$ZnAs_2\ (s) + 2\ Zn\ (s) = Zn_3As_2\ (s) \quad (7)$$

It is evident that the virtual-cell reaction (6) is the reaction of the formation of the $ZnAs_2$ compound from elementary components. Therefore, the corresponding partial molar functions of zinc in the $ZnAs_2$ + As two-phase field are thermodynamic functions of the formation of 1 mole of the $ZnAs_2$ compound.

According to equation (6) the absolute entropy of the $ZnAs_2$ compound was calculated according to the equation given below:

$$S^0(ZnAs_2) = \overline{\Delta S}_{Zn} + S^0\ (Zn) + 2S^0(As) \quad (8)$$

The standard Gibbs free energy, enthalpy and entropy of formation of the Zn_3As_2 compound were calculated using the following equations in accordance with the reaction (7):

$$\Delta_f Z^0(Zn_3As_2) = 2\Delta\overline{Z}_{Zn} + \Delta_f Z^0(ZnAs_2) \quad (9)$$

where $Z \approx G, H$ *or* S.

Absolute entropy of the Zn_3As_2 compound was calculated using the following equation:

$$S^0(Zn_3As_2) = 2 \cdot [\Delta\overline{S}_{Zn} + S^0(Zn)] + S^0(ZnAs_2) \quad (10)$$

Errors were calculated by the error accumulation method. Absolute entropies of the elementary zinc and arsenic used for calculations were taken from (Iorish & Yungman, 2006): $S^0(Zn) = 41.63 \pm 0.13$ J/(mole · K); $S^0(As) = 35.61 \pm 0.04$ J/(mole · K). Calculated standard integral thermodynamic functions of both compounds along with literature data are summarized in Table 5.

Table 5. A comparative table analyzing the standard integral thermodynamic functions of $ZnAs_2$ and Zn_3As_2 compounds, combining results from this study and available literature data

Compound	$-\Delta_f G^0$	$-\Delta_f H^0$	$\Delta_f S^0$	S^0	*Reference, method*
	kJ · mol⁻¹		*J · mol⁻¹ · K⁻¹*		
$ZnAs_2$	60.97 ± 0.1	66.2 ± 0.5	- 17.6 ± 1.2	95.3 ± 1.3	This work, EMF
	64.433	73.22		83.374	(Iorish & Yungman, 2006), recomm.
		41.8			(Wagman *et al*., 1967), recomm.
	64.64 ± 3.35	73.64 ± 1.67	- 30.54 ± 1.67	82.3	(Sirota & Sklyarenko, 1968), EMF
		78.66			(Silvey *et al*., 1961), vapor pres.
		78.66	18.5		(Lyons, 1959), vapor pres.
		81.59		84.17	(Jordan, 1971), vapor press.
Zn_3As_2	126.2 ± 0.3	135.5 ± 1.1	- 31.3 ± 3.2	164.8 ± 3.5	This work, EMF
	125.52	133.89		168.037	(Iorish & Yungman, 2006), recomm.
	125.46	133.89		168.04	(Barin, 2008), recomm.
		134.7 ± 10.5		165.3 ± 11.7	(Kubaschewski *et al*., 1967), recomm.
		32.2			(Wagman *et al*., 1967), recomm.
	125.94 ± 7.1	136.4 ± 5.0	- 35.56 ± 6.7	160.6	(Sirota & Sklyarenko, 1968), EMF
		141.9		196.65	(Jordan, 1971), vapor press.
		121.33			(Shchukarev *et al*.,1955), calorimetry
		127.6			(Ariya *et al*., 1957), calorimetry
		143.4			(Binnewies & Milke, 2002), recomm.
		126.8			(Natta & Passerini, 1928), calorimet.
	122.2				(Stull & Sinke, 1956), calorimetry
		127.6			(Greenberg *et al*., 1985), vapor pres.

As presented in the table, the values of standard Gibbs free energy ($-\Delta fG_0$) and enthalpy of formation ($-\Delta fH_0$) for the $ZnAs_2$ compound calculated in the present work stand out as the most precise and reliable data compared to the available literature. The low deviation observed in these values highlights their high accuracy and demonstrates the careful handling of experimental conditions and computational methods used in this study. This minimal deviation ensures that the thermodynamic parameters provided here

are more trustworthy, offering a more reliable foundation for future research and practical applications involving zinc arsenides. In most other works, except for (Sirota & Sklyarenko, 1968) and (Kubaschewski et al., 1967), the error of the quantities is not mentioned, which in turn reduces their accuracy.

The enthalpy of formation values provided in studies (Silvey *et al*., 1961; Lyons, 1959; Jordan, 1971) are not direct experimental results but rather values calculated indirectly and are relatively higher. The lower value of standard enthalpy of formation (41.8 kJ/mol) given in (Wagman *et al*., 1967) is a notable outlier and likely results from differences in experimental assumptions or conditions. A comprehensive thermodynamic study of $ZnAs_2$ has been conducted only in (Sirota & Sklyarenko, 1968) using high temperature EMF measurements and by us in the present study. The Δ_fG^0 and Δ_fH^0 values determined in our study are lower than those reported in (Sirota & Sklyarenko, 1968). It is worth mentioning that, unlike the approach in (Sirota & Sklyarenko, 1968) our experiments were conducted using a low-temperature EMF method, which is regarded as more accurate because it minimizes the need for extensive extrapolation of results to standard condition.

Similar to the $ZnAs_2$ compound, a comprehensive thermodynamic study of the Zn_3As_2 compound has only been conducted by the authors of (Sirota & Sklyarenko, 1968) and in the present work (Table 5). The results obtained are in good agreement with one another. Overall, the literature data on the standard Gibbs free energy of formation for Zn_3As_2 show minimal variation and the values we have determined largely confirm these findings.

However, the same cannot be said for the standard enthalpy of formation values for this compound. The Δ_fH^0 values for Zn_3As_2 generally fall within a range of approximately 120 to 140 kJ/mol, with only one notable outlier. The lowest value (32.2 kJ/mol) reported originates from the same study (Wagman *et al*., 1967) constituting an exception to $ZnAs_2$. The Δ_fH^0 value determined in our work closely aligns with the value obtained from high-temperature EMF measurements (Sirota & Sklyarenko, 1968). Additionally, the enthalpy of formation values provided in the (Iorish & Yungman, 2006; Barin, 2008; Kubaschewski *et al*., 1967; Wagman *et al*., 1967) directories are assessments derived based on EMF studies and show strong agreement with our findings.

It should be noted that the analysis of the scientific literature shows that the formation Gibbs free energy, formation entropy and absolute entropy of zinc arsenides have been poorly studied in relation to standard enthalpy. This, in turn, reduces the possibility of conducting a comprehensive comparative analysis in this field. The absolute entropy obtained by us for this compound is generally consistent with existing literature data. The values obtained for the $ZnAs_2$ compound in our study are slightly higher than those of the other three results. For the other compound - Zn_3As_2, the value presented in this work shows good agreement with most of the literature data. The only discrepancy is a significantly higher value (196.65 J/mol·K) of S^0 calculated using the vapor pressure measurement method.

The fundamental thermodynamic quantities obtained in this study provide a comprehensive basis for analyzing the stability of zinc arsenides, their behavior in chemical and industrial processes under varying conditions and for selecting optimal compositions when preparing these phases. The thermodynamic data sets obtained using the low-temperature EMF method are highly accurate and effectively resolve existing discrepancies in the literature regarding the thermodynamic properties of these compounds. As such, this work makes a significant contribution to advancing scientific

understanding in the field. The fundamental thermodynamic parameters of zinc arsenides derived from this study can be integrated into modern electronic databases and handbooks, offering valuable resources for future thermodynamic studies of systems involving these materials.

4. Conclusion

In this study, we present the results of a thermodynamic investigation of zinc antimonides using the low-temperature EMF method with a glycerol electrolyte, conducted within a temperature range of 300 to 440 K. By employing samples from the $ZnAs_2$ + As and Zn_3As_2 + $ZnAs_2$ two-phase regions as the right electrodes, linear equations describing the temperature dependence of the EMF were derived. From these equations, the partial molar thermodynamic functions of zinc in the alloys were calculated. Potential-generating reactions for both binary compounds were identified using the T-x diagram of the Zn-As system, enabling the determination of their standard integral thermodynamic functions. Presented mutually consistent thermodynamic values are the first experimental data derived from the EMF measurements near standard conditions. These standard thermodynamic values are highly precise and contribute significantly to the understanding of zinc arsenides' thermodynamics, helping to reconcile discrepancies in the existing literature.

References

Ali, A., Anwar, A.W., Moin, M., Babar, M. & Thumu, U. (2024). Investigation of structural, mechanical, electronic and optical responses of Ga doped aluminum arsenide for optoelectronic applications: By first principles. *Heliyon*, *10*(2). https://doi.org/10.1016/j.heliyon.2024.e24597

Aliev, Z.S., Musaeva, S.S., Babanly, D.M., Shevelkov, A.V. & Babanly, M.B. (2010). Phase diagram of the Sb-Se-I system and thermodynamic properties of SbSeI. *Journal of Alloys and Compounds*, *505*(2), 450-455. https://doi.org/10.1016/j.jallcom.2010.06.103

Aliev, Z.S., Musayeva, S.S., Imamaliyeva, S.Z. & Babanly, M.B. (2018). Thermodynamic study of antimony chalcoiodides by EMF method with an ionic liquid. *Journal of Thermal Analysis and Calorimetry*, 133, 1115-1120. https://doi.org/10.1007/s10973-017-6812-4

Aliyev, F.R., Orujlu, E.N., Mashadiyeva, L.F., Dashdiyeva, G.B. & Babanly, D.M. (2024). Solid-phase equilibria and thermodynamic properties of the Sb-Te-S system. *Physics and Chemistry of Solid State*, *25*(1), 26-34. https://doi.org/10.15330/pcss.25.1.26-34

Ariya, S.M., Morozova, M.P., Khuan, T.T. & Vol'f, E. (1957). Enthalpy of formation of arsenides of lithium and zinc. *Journal of General Chemistry*, 27, 293-295. (In Russian).

Babanly, D.M., Aghayeva, A.R., Mammadova, S.H. & Tagiyev, D.B. (2024). Thermodynamic study of the CdSb compound by the electromotive force measurements method. *Chemical Problems*, *22*(4), 402-410. https://doi.org/10.32737/2221-8688-2024-4-402-410

Babanly, D.M., Aghayeva, A.R., Mirzayev, R.E., Mashadiyeva, L.F. & Jafarov, Y.I. (2025). Thermodynamic study of copper antimonides by the EMF method with the $Cu_4RbCl_3I_2$ solid electrolyte. *Russian Journal of Physical Chemistry A*, *98*(14), 3266-3272.

Babanly, M.B., Tedenac, J.C., Aliyev, Z.S. & Balitsky, D.V. (2009). Phase equilibriums and thermodynamic properties of the system Bi-Te-I. *Journal of Alloys and Compounds*, *481*(1-2), 349-353. https://doi.org/10.1016/j.jallcom.2009.02.139

Babanly, M.B., Yusibov, Y.A. & Babanly, N.B. (2011). The EMF method with solid-state electrolyte in the thermodynamic investigation of ternary copper and silver chalcogenides. *Electromotive Force and Measurement in Several Systems*, 57-78. https://doi.org/10.5772/28934

Babanly, M.B., Yusibov, Y.A. (2011). *Electrochemical Methods in Thermodynamics of Inorganic Systems*. Baku: Science.

Babanly, N.B., Orujlu, E.N., Imamaliyeva, S.Z., Yusibov, Y.A. & Babanly, M.B. (2019). Thermodynamic investigation of silver-thallium tellurides by EMF method with solid electrolyte Ag_4RbI_5. *The Journal of Chemical Thermodynamics*, 128, 78-86. https://doi.org/10.1016/j.jct.2018.08.012

Barin, I. (2008). *Thermochemical Data of Pure Substances*, 3rd edition. Wiley-VCH.

Binnewies, M., Milke, E. (2002). *Thermochemical Data of Elements and Compounds*, 2. Weinheim: Wiley-VCH. https://doi.org/10.1002/9783527618347

Buschow, K.H.J., Cahn, R.W. (2001). *Encyclopedia of Materials. Science and Technology*, 2nd edition. https://doi.org/10.1016/B978-0-08-043152-9.X5000-1

Colegrove, E., Albin, D.S., Moutinho, H.R., Amerasinghe, M., Burst, J.M., Metzger, W.K. (2020). Scalable ultrafast epitaxy of large-grain and single-crystal II-VI semiconductors. *Scientific Reports*, *10*(1), 2426. https://doi.org/10.1038/s41598-020-59083-3

Crow, J.D., Comerford, L.D., Harper, J.S., Brady, M.J. & Laff, R.A. (1978). Gallium arsenide laser-array-on-silicon package. *Applied Optics*, *17*(3), 479-485. https://doi.org/10.1364/AO.17.000479

Galstyan, V.G., Deigen, M.I., Muratova, V.I., Semiletov, A., Stankevich, V.C. & Tikhonova, A.A. (1991). Relation between growth conditions, structure and cathodoluminescence of epitaxial layers of ZnSe on GaAs. In *Growth of Crystals*, 16, 127-140. https://doi.org/10.1007/978-1-4615-3662-8_9

Ghasemi, M., Johansson, J. (2015). Thermodynamic assessment of the As-Zn and As-Ga-Zn systems. *Journal of Alloys and Compounds*, 638, 95-102. https://doi.org/10.1016/j.jallcom.2015.03.051

Greenberg, J.H., Guskov, V.N. & Lazarev, V.B. (1985). Vapour-pressure investigation of thermodynamics of non-stoichiometric crystals. Sublimation of β-Zn_3As_2. *The Journal of Chemical Thermodynamics*, *17*(8), 739-746. https://doi.org/10.1016/0021-9614(85)90103-X

Hnuna, L., Haidar, E.A., Djamel, B., Stampfl, C., Mohammed, S. & Pachuau, Z. (2023). First-principles study of optical and thermoelectric properties of Zn_3As_2 and ZnSb. *Nano Select*, *4*(9-10), 551-558. https://doi.org/10.1002/nano.202300074

Iorish, V.S., Yungman, V.S. (2006). Thermal constants of substances: Database.

Ipser, H., Mikula, A. & Katayama, I. (2010). Overview: The emf method as a source of experimental thermodynamic data. *Calphad*, *34*(3), 271-278. https://doi.org/10.1016/j.calphad.2010.05.001

Islam, M.M., Kauzlarich, S.M. (2023). The potential of arsenic-based Zintl phases as thermoelectric materials: Structure & thermoelectric properties. *Journal of Inorganic and General Chemistry*, *649*(21), e202300149. https://doi.org/10.1002/zaac.202300149

Jalali, H.B., De Trizio, L., Manna, L. & Di Stasio, F. (2022). Indium arsenide quantum dots: An alternative to lead-based infrared emitting nanomaterials. *Chemical Society Reviews*, *51*(24), 9861-9881. https://doi.org/10.1039/D2CS00490A

Jordan, A.S. (1971). Some thermodynamic properties of Zn_3As_2, Cd_3As_2 and ZnP_2. *Journal of The Electrochemical Society*, *118*(8), 1362.

Kaur, M., Sharma, G., Rérat, M. & Joshi, K.B. (2020). Computational analysis of strain-induced electronic and optical properties of Zn_3As_2. *Journal of Materials Science*, *55*(12), 5099-5110. https://doi.org/10.1007/s10853-019-04331-9

Khan, A.U.R., Ramzan, M., Iqbal, M.F., Hafeez, M., Fadhali, M.M., Somaily, H.H., ... & Saleem, M.F. (2022). Effect of the source-to-substrate distance on structural, optoelectronic and thermoelectric properties of zinc sulfide thin films. *Materials*, *15*(22), 8047. https://doi.org/10.3390/ma15228047

Kidari, O., Chartrand, P. (2023). Thermodynamic evaluation and optimization of the As-Cd, As-Zn and As-Cd-Zn Systems. *Metallurgical and Materials Transactions B*, *54*(5), 2793-2814. https://doi.org/10.1007/s11663-023-02875-5

Kim, S., Lee, K., Gwak, N., Shin, S., Seo, J., Noh, S.H., ... & Oh, N. (2024). Colloidal synthesis of p-type Zn_3As_2 nanocrystals. *Advanced Materals*, *36*(21), 2310671. https://doi.org/10.1002/adma.202310671

Kozlov, A.I., Kozlova, S.G., Matveev, A.V. & Sobolev, V.V. (2002). Parameters of excitons in monoclinic zinc diarsenide. *Semiconductors*, 36, 755-757. https://doi.org/10.1134/1.1493744

Lazarev, V., Marenkin, S.F., Maksimova, S.I., Hkuseinov, B. & Shevchenko, V.Y. (1979). The region of homogeneity of $ZnAs_2$. *Izvestiya Akademii Nauk SSSR, Neorganicheskie Materialy*, *15*(5), 586-587.

Lazarev, V.B., Guskov, V.N. & Greenberg, J.H. (1981). PTX phase equilibria in the system Zn-As. *Materials Research Bulletin*, *16*(9), 1113-1120. https://doi.org/10.1016/0025-5408(81)90287-7

Lyons, V.J. (1959). The dissociation pressure of $ZnAs_2$. *The Journal of Physical Chemistry*, *63*(7), 1142-1144. https://doi.org/10.1021/j150577a026

Mashadieva, L.F., Babanly, D.M., Yusibov, Y.A., Tagiev, D.B. & Babanly, M.B. (2021a). Thermodynamic study of the Ag-Sb-Se system by the EMF method with Ag_4RbI_5 solid electrolyte. *Russian Journal of Electrochemistry*, *57*(3), 281-288. https://doi.org/10.1134/S1023193521030083

Mashadiyeva, L.F., Mammadli, P.R., Babanly, D.M., Ashirov, G.M., Shevelkov, A.V. & Yusibov, Y.A. (2021b). Solid-phase equilibria in the Cu-Sb-S system and thermodynamic properties of copper-antimony sulfides. *JOM*, 73, 1522-1530. https://doi.org/10.1007/s11837-021-04624-y

Morachevsky, A., Voronin, G., Geyderich, V. & Kutsenok, I. (2003). *Electrochemical Research Methods in Thermodynamics of Metal Systems*. Moscow: Akademkniga Publisher, 334. https://elibrary.ru/item.asp?id=19603291 (In Russian).

Moroz, M., Demchenko, P., Prokhorenko, M., Reshetnyak, O. & Tesfaye, F. (2024). Phase equilibria and thermodynamic properties of compounds in the Ag_2FeS_2-Ga_2S_3 cross-section of the Ag-Fe-Ga-S system determined by the EMF method. *JOM*, 1-8. https://doi.org/10.1007/s11837-024-07024-0

Natta, G., Passerini, L. (1928). Compounds of arsenic with magnesium and zinc. *Gazzetta Chimica Italiana*, 58, 541-550.

Nigl, T.P., Smith, N.D., Lichtenstein, T., Gesualdi, J., Kumar, K. & Kim, H. (2017). Determination of thermodynamic properties of alkaline earth-liquid metal alloys using the electromotive force technique. *Journal of Visualized Experiments: JoVE*, 129, 56718. https://doi.org/10.3791/56718

Okamoto, H. (1992). The As-Zn (arsenic-zinc) system. *Journal of Phase Equilibria*, 13, 155-161. https://doi.org/10.1007/BF02667479

Rajpurohit, S., Sharma, G. (2023). Ab-initio investigation of elastic properties of monoclinic $ZnAs_2$ crystal. *Journal of Condensed Matter*, *1*(2), 56-60. https://doi.org/10.61343/jcm.v1i02.34

Shao, Y. (2012). *Electrochemical Cells: New Advances in Fundamental Research and Applications*. BoD - Books on Demand.

Shchukarev, S.A., Grossman, G.A. & Morozova, M.P. (1955). Enthalpy of formation of zinc phosphide Zn_3P_2. *Journal of General Chemistry*, *25*(4), 633-634. (In Russian).

Sicius, H. (2024). Semiconductors. In *Handbook of the Chemical Elements*. Springer, Berlin, Heidelberg. https://doi.org/10.1007/978-3-662-68921-9_23

Silvey, G.A., Lyons, V.J. & Silvestri, V.J. (1961). The preparation and properties of some II–V semiconducting compounds. *Journal of the Electrochemical Society*, *108*(7), 653.

Sirota, N.N., Sklyarenko, E.M. (1968). Thermodynamic properties of compounds in the Zn-As and Sd-As systems. *Russian Metallurgy (Metally)*, 5, 159-161.

Stamov, I.G., Syrbu, N.N., Ursaki, V.V. & Dorogan, A.V. (2012). Energy band structure and optical constants of $ZnAs_2$ crystals. *Optics Communications*, *285*(13-14), 3104-3110. https://doi.org/10.1016/j.optcom.2012.02.047

Stamov, I.G., Tkachenko, D.V. & Strel'chuk, Y. (2022). Characteristics of surface-barrier structures on Zinc diarsenide with hole conductivity. In *5th International Conference on Nanotechnologies and Biomedical Engineering: Proceedings of ICNBME-2021*, 92-99. Springer International Publishing. https://doi.org/10.1007/978-3-030-92328-0_13

Stoyko, S.S., Mar, A. (2011). Ternary rare-earth zinc arsenides $REZn_{1-x}As_2$ (RE= La-Nd, Sm). *Journal of Solid State Chemistry*, *184*(9), 2360-2367. https://doi.org/10.1016/j.jssc.2011.07.002

Stull, D.R., Sinke, G.C. (1956). *Thermodynamic Properties of the Elements.* Publisher: American Chemical Society.

Stutz, E.Z., Friedl, M., Burgess, T., Tan, H.H., Caroff, P., Jagadish, C. & Fontcuberta i Morral, A. (2019). Nanosails showcasing Zn_3As_2 as an optoelectronic-grade earth abundant semiconductor. *physica status solidi (RRL)-Rapid Research Letters*, *13*(7), 1900084. https://doi.org/10.1002/pssr.201900084

Vurgaftman, I., Meyer, J.A.R. & Ram-Mohan, L.R. (2001). Band parameters for III-V compound semiconductors and their alloys. *Journal of Applied Physics*, *89*(11), 5815-5875. https://doi.org/10.1063/1.1368156

Wagman, D.D., Evans, W.H., Parker, V.B., Schumm, R.H., Halo R.H.I., Bailey, S.M., … & Neutral, J. (1967). Table 34: Cadmium. In *Selected Values of Chemical Thermodynamic Properties*. National Bureau of Standards, Washington, D.C.

Zakhvalinskii, V.S., Nikulicheva, T.B., Pilyuk, E.A., Kubankin, A.S. & Morocho, A.A. (2021). Calculation of the band structure and density of localized states of materials of the quasi-binary system Zn_3As_2-Mn_3As_2. *Solid State Communications*, 328, 114237. https://doi.org/10.1016/j.ssc.2021.114237

Kubaschewski, O., Evans, E.L. & Alcock, C.B. (1967). *Metallurgical Thermochemistry*, 4th edition. Pergamon Press.